Divalent Cation-, Nucleotide-, and Polymerization-Dependent Changes in the Conformation of Subdomain 2 of Actin

Joanna Moraczewska,* Barbara Wawro,* Katsuya Seguro,# and Hanna Strzelecka-Gołaszewska*
*Department of Muscle Biochemistry, Nencki Institute of Experimental Biology, PL-02-093 Warsaw, Poland, and #Food Research and Development Laboratories, Ajinomoto Co., Suzuki-cho, Kawasaki-ku, Kawasaki, Kanagawa 210, Japan

ABSTRACT Conformational changes in subdomain 2 of actin were investigated using fluorescence probes dansyl cadaverine (DC) or dansyl ethylenediamine (DED) covalently attached to Gln^{41}. Examination of changes in the fluorescence emission spectra as a function of time during Ca^{2+}/Mg^{2+} and ATP/ADP exchange at the high-affinity site for divalent cation-nucleotide complex in G-actin confirmed a profound influence of the type of nucleotide but failed to detect a significant cation-dependent difference in the environment of Gln^{41}. No significant difference between Ca- and Mg-actin was also seen in the magnitude of the fluorescence changes resulting from the polymerization of these two actin forms. Evidence is presented that earlier reported cation-dependent differences in the conformation of the loop 38–52 may be related to time-dependent changes in the conformation of subdomain 2 in DED- or DC-labeled G-actin, accelerated by substitution of Mg^{2+} for Ca^{2+} in CaATP-G-actin and, in particular, by conversion of MgATP- into MgADP-G-actin. These spontaneous changes are associated with a denaturation-driven release of the bound nucleotide that is promoted by two effects of DED or DC labeling: lowered affinity of actin for nucleotide and acceleration of ATP hydrolysis on MgATP-G-actin that converts it into a less stable MgADP form. Evidence is presented that the changes in the environment of Gln^{41} accompanying actin polymerization result in part from the release of P_i after the hydrolysis of ATP on the polymer. A similarity of this change to that accompanying replacement of the bound ATP with ADP in G-actin is discussed.

INTRODUCTION

It is well known that the type of nucleotide, ATP or ADP, and the type of divalent cation, Ca^{2+} or Mg^{2+}, bound with high affinities in the cleft between the two domains of the actin monomer (Kabsch et al., 1990), influence the kinetics of actin polymerization and dynamic properties of actin filaments (for a review, see Carlier, 1991; Estes et al., 1992). These effects might be exerted through transmission of conformational changes from the binding site for the cation-nucleotide complex to the surface loops participating in the intermonomer interactions, and/or by influencing the relative orientation of the domains or subdomains of the monomer. That actin can adopt different conformations by relative movements of the two domains and their subdomains about hinge points has been concluded from normal mode analysis of G-actin (Tirion and ben-Avraham, 1993) and experimentally proved by crystallographic analysis of β-actin:profilin complex under different chemical or physical conditions (Chik et al., 1996).

There is growing evidence that changes in the orientation of subdomain 2 of actin and conformational transitions within this subdomain may play important roles in the polymerization process and stabilization of the filament. The atomic models of F-actin (Holmes et al., 1990; Lorenz et al., 1993; Tirion et al., 1995) as well as the ribbon structure of β-actin:profilin crystals (Schutt et al., 1993) implicate the DNase I–binding loop (residues 38–52) on the surface of subdomain 2 in formation of actin-actin contacts, consistent with the inhibition of actin polymerization by certain chemical or proteolytic modifications of this loop (Hegyi et al., 1974; Schwyter et al., 1989; Khaitlina et al., 1993). Refinements of the atomic model of F-actin against data obtained from low-resolution x-ray diffraction on oriented F-actin gels (Lorenz et al., 1993; Tirion et al., 1995) suggest that polymerization of CaATP-G-actin is accompanied by a rotation and shift of subdomain 2 toward subdomain 4 and reorientation of loop 38–52 relative to the G-actin:DNase I crystal structure. Narrowing of the interdomain cleft resulting from these changes has been confirmed by fluorescence resonance energy transfer measurements (Miki and Kouyama, 1994). Studies on F-actin trapped in an ADP-P_i state that use beryllium fluoride as an analog of inorganic phosphate showed that some of these alterations may be linked to the release of P_i after hydrolysis of the actin-bound ATP that accompanies polymer growth. The differences in the structure of subdomain 2 in the filaments in the ADP-P_i state and in the final ADP state, revealed by three-dimensional reconstructions of the filaments from electron micrographs (Orlova and Egelman, 1992) and by limited proteolysis experiments (Muhlrad et al., 1994), were suggested to be a structural basis for the earlier demonstrated destabilization of the polymer by P_i release from the ADP-P_i intermediate (references in Carlier, 1991). Conformational transitions in subdomain 2 of monomeric actin that may be related to the regulation of actin polymerization by the type of the bound nucleotide, ATP or ADP (references in Carlier, 1991; Estes et al., 1992), have

Received for publication 30 June 1998 and in final form 25 February 1999.
Address reprint requests to Dr. Hanna Strzelecka-Gołaszewska, Department of Muscle Biochemistry, Nencki Institute of Experimental Biology, 3 Pasteur Street, PL-02-093 Warsaw, Poland. Tel.: 48-22-6686182; Fax: 48-22-225342; E-mail: hannas@nencki.gov.pl.

0006-3495/99/07/373/13 $2.00

also been detected. Profound changes in the conformation of the DNase I–binding loop were revealed by limited proteolysis (Strzelecka-Gołaszewska et al., 1993; Muhlrad et al., 1994), fluorescence measurements on actin labeled at Gln^{41} with dansyl ethylenediamine (DED) or dansyl cadaverine (DC) (Kim et al., 1995; Moraczewska et al., 1996), and changes in the ability of Gln^{41} of G-actin to participate in a cross-link formation with S1 in a bacterial transglutaminase-catalyzed reaction (Eligula et al., 1998). The proteolytic digestion experiments also demonstrated a sensitivity of the segment 61–69 to ATP/ADP replacement in G-actin. Similar studies on the effects of Ca^{2+}/Mg^{2+} replacement at the high-affinity site for divalent cation resulted in divergent findings. A profound change in the environment of Gln^{41}, apparent from measurements of the fluorescence of DED-labeled G-actin (Kim et al., 1995), has not been observed with DC-labeled actin (Moraczewska et al., 1996). Likewise, the sensitivity of subtilisin cleavage at Met^{47} to the type of the bound cation reported by Kim et al. (1995) is in disagreement with earlier limited proteolysis studies showing conformational effects of Ca^{2+}/Mg^{2+} replacement in G-actin on the segment 61–69 but not on the DNase I–binding loop (Strzelecka-Gołaszewska et al., 1993). Examination of cation-dependent differences in the structure of subdomain 2 in the polymer subunits by comparison of electron microscopic three-dimensional reconstructions of the filaments of Ca- and Mg-F-actin have also led to controversial findings (Orlova and Egelman, 1993; Steinmetz et al., 1997).

In view of the suggested participation of the loop 38–52 in the intermonomer contacts in F-actin, clarification of possible influence of the type of the tightly bound cation on the conformation of this loop in both G- and F-actin seems to be important for at least two reasons: 1) the atomic models of F-actin were based on the structure of this protein with Ca^{2+} bound at the high-affinity site, whereas Mg^{2+} is the in vivo bound cation (references in Estes et al., 1992); 2) cation-dependent changes in the conformation of the loop 38–52 might be a structural basis for the differences in the kinetics of polymerization of Ca- and Mg-actin and in the dynamics of their filaments (Carlier, 1991; Estes et al., 1992; Orlova and Egelman, 1993). In this study we present new data on the cation-, nucleotide-, and polymerization-dependent changes in the environment of Gln^{41} probed with dansyl fluorophores attached to this residue. By direct comparison of changes in the fluorescence of DED- and DC-labeled actin, we have excluded the possibility that the discrepancies between the earlier observations arise from different orientation of the fluorophore in DED- and DC-actin due to a longer linker arm in DC. The data presented here document that the environment of Gln^{41} in both G- and F-actin is not significantly influenced by the type of cation, Ca^{2+} or Mg^{2+}, present at the high-affinity site and suggest that the earlier reported differences between Ca- and Mg-G-actin, as well as the difference between changes accompanying polymerization of these two forms of actin (Kim et al., 1995), may be related to spontaneous time-dependent changes in the fluorescence spectra of DED- or DC-labeled actin. Evidence is presented that these spontaneous changes, relatively slow in CaATP-G-actin but largely accelerated by transformation of CaATP- into MgATP-G-actin and by further replacement of ATP with ADP, reflect profound changes in the conformation of subdomain 2 upon release of the bound nucleotide and are associated with diminished affinity of DED- or DC-modified G-actin for nucleotide.

MATERIALS AND METHODS

Reagents

DC (dansyl cadaverine) and DED (dansyl ethylenediamine) were purchased from Molecular Probes (Eugene, OR). ATP, ADP, hexokinase, and EGTA were from Sigma Chemical Co (St. Louis, MO).

Protein preparation and labeling

Rabbit skeletal muscle actin was prepared as described by Spudich and Watt (1971) and was stored in buffer containing 2 mM HEPES (pH 7.6), 0.2 mM ATP, 0.1 mM $CaCl_2$, 0.2–0.4 mM DTT, and 0.02% NaN_3 (buffer G) at 2°C. Unless stated otherwise, before measurements the concentration of $CaCl_2$ was lowered to 50 μM by dilution of actin with a Ca^{2+}-free buffer G.

Labeling of Gln^{41} of actin with DC or DED in the reaction catalyzed by transglutaminase was performed using Ca^{2+}-independent microbial transglutaminase obtained and purified as described by Huang et al. (1992). Actin (24 μM) in buffer G was incubated with transglutaminase (0.5–1.0 unit/ml) and either DC or DED equimolar to actin, for 2 h at room temperature. To remove the enzyme and unbound label, actin was polymerized with 0.1 M KCl, and F-actin was collected by ultracentrifugation at 150,000 $\times$ g for 1.5 h and then depolymerized by exhaustive dialysis against buffer G. To remove the remaining unbound label and some cross-linked actin oligomers produced by the reaction with transglutaminase, DC- and DED-labeled actins were gel-filtered on a Sephadex G-100 column, and buffer G was used as the eluent. Before use, actin solutions were clarified by centrifugation at 100,000 $\times$ g for 1 h at 4°C.

MgATP-G-actin was prepared directly before measurements by incubation of CaATP-G-actin with 0.2 mM EGTA/0.05 mM $MgCl_2$ for 3 min at 25°C after the initial concentration of Ca^{2+} ions was lowered to 50 μM by dilution of actin with a Ca^{2+}-free buffer G. This treatment ensures complete replacement of the initially bound Ca^{2+} with Mg^{2+} (Gershman et al., 1986).

MgADP-G-actin was prepared essentially as described by Gershman et al. (1989), by incubation of MgATP-G-actin with 0.8 mM ADP, 0.3 mM glucose, and hexokinase (20 U/ml) to convert the initially present ATP (0.2 mM) into ADP, at 0°C for ~1 h.

The concentration of G-actin was determined spectrophotometrically, using an absorption coefficient of 0.63 mg ml^{-1} at 290 nm (Houk and Ue, 1974). The contribution of the label to the total absorption at 290 nm was negligible. The labeling ratios were determined spectrophotometrically, using a molar absorption coefficient of 4.64×10^3 M^{-1} cm^{-1} at 326 nm for DC (Lorand et al., 1968) and 4.8×10^3 M^{-1} cm^{-1} at 334 nm for DED (Kim et al., 1995).

Fluorescence and light-scattering measurements

Fluorescence and light-scattering measurements were carried out in a Spex Fluorolog spectrofluorometer (Spex Industries, Edison, NJ).

ATP hydrolysis

ATP hydrolysis during storage of actin in the MgATP form was assayed by determination of inorganic phosphate by the malachite green method (Kodama et al., 1986).

Determination of exposed thiol groups

Exposed thiol groups were determined spectrophotometrically by reaction with 0.25 mM β-hydroxyethyl-2,4-dinitrophenyl disulfide (HEDD), using a value of 13,060 M^{-1} cm^{-1} at 408 nm for an absorption coefficient of 2,4-dinitrothiophenol released in this reaction (Bitny-Szlachto, 1960). Actin used for thiol group titrations was exhaustively dialyzed against DTT-free buffer G. In the course of EDTA-induced denaturation of actin, the fast initial reaction with HEDD of the already exposed groups (complete in less than 1 min) was followed by a slower process reflecting the denaturation-driven uncovering of other thiol groups. The number of thiol groups exposed after any given time of incubation with EDTA was calculated by extrapolation of the second portion of the reaction progress curve to the time of the addition of HEDD (time 0 for the reaction with HEDD).

Kinetic data analysis

The kinetic parameters for the data shown in this paper were computed by nonlinear regression with the Levenberg-Marquardt algorithm (program Curve Expert 1.3).

RESULTS

Effects of exchange of the tightly bound Ca^{2+} for Mg^{2+} on the environment of Gln^{41} in G-actin

The disparate findings with regard to the effects of Ca^{2+}/Mg^{2+} exchange on the environment of Gln^{41} in G-actin probed using DED- (Kim et al., 1995) or DC-labeled actin (Moraczewska et al., 1996) prompted us to more carefully examine these effects. This was done by following time courses of changes in the fluorescence of labeled CaATP-G-actin after the addition of 0.2 mM EGTA/0.05 mM $MgCl_2$ to initiate an exchange of the bound Ca^{2+} for Mg^{2+}. As shown in Fig. 1 *A* for DED-labeled actin, the addition of EGTA/$MgCl_2$ resulted in a ~3% decrease in the fluorescence intensity. No significant shift in position of the fluorescence maximum was detected. The half-time of this transition, ~40 s at 25°C, is in good agreement with the kinetics of Ca^{2+} release from CaATP-G-actin, which is the rate-limiting step in the conversion of Ca-G-actin into Mg-G-actin (Estes et al., 1987; Nowak et al., 1988). Thus the initial quenching of the fluorescence appears to be linked to the replacement of the bound Ca^{2+} with Mg^{2+}. This change was followed, however, by a slow increase in the fluorescence intensity and a blue shift of the fluorescence maximum (Fig. 1 *B*). Similar transitions were observed with DC-labeled actin (data not illustrated). These observations explain why the previously reported spectra of DC-labeled MgATP-G-actin (Moraczewska et al., 1996), which were recorded after 10–15 min of incubation of CaATP-G-actin with EGTA/$MgCl_2$ at 20°C, revealed a small (~5%) increase rather than the decrease in the fluorescence intensity. The spectra reported by Kim et al. (1995) for DED-labeled MgATP-G-actin are characteristic of a later stage of the slow transformation of this actin into another conformational state, which might result from a longer storage of actin in the Mg form before the measurement.

An increase in the fluorescence intensity and a blue shift of the emission maximum of both DED- and DC-labeled G-actin have been observed when the bound ATP was replaced with ADP (Kim et al., 1995; Moraczewska et al., 1996). In light of these findings, it was reasonable to suppose that one of the reasons for the changes occurring during storage of G-actin in the MgATP form might be the slow hydrolysis of the bound ATP reported to take place in this form of actin (Attri et al., 1991; Mossakowska et al., 1993). As shown in Fig. 2, a 66% labeling of actin with DED further increased the rate of ATP hydrolysis, from ~0.3 to ~0.5 mol/mol actin/h at 25°C. This may be an

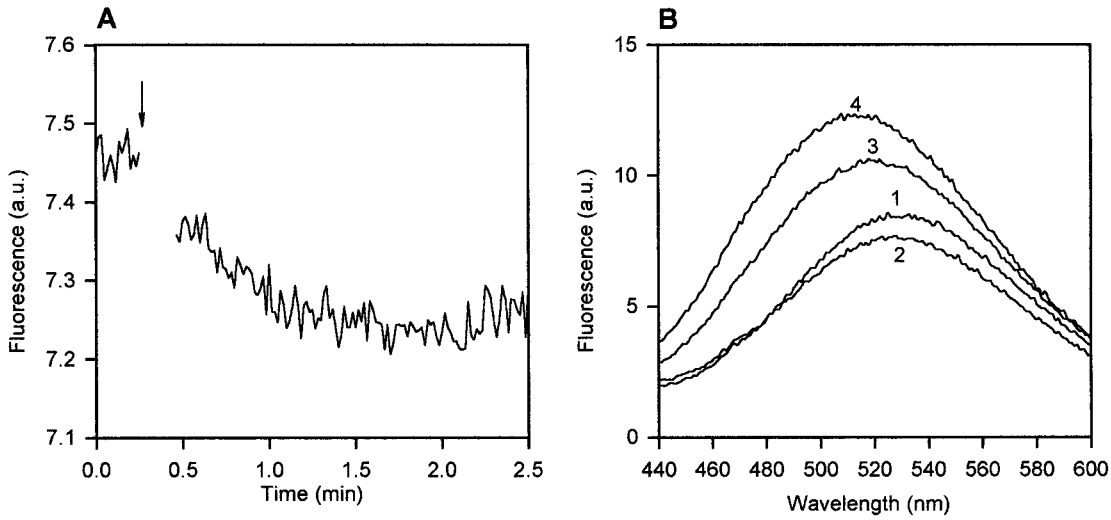

FIGURE 1 Effects of exchange of the tightly bound Ca^{2+} for Mg^{2+} on the fluorescence of DED-labeled G-actin. (*A*) Time course of changes in the fluorescence of DED-G-actin after the addition of 0.2 mM EGTA/50 μM $MgCl_2$ (*arrow*) to CaATP-G-actin (1 μM, 83% DED-labeled) at 25°C. The fluorescence intensity was registered at 525 nm after excitation at 344 nm. (*B*) Fluorescence emission spectra of DED-labeled CaATP-G-actin (*trace 1*), and of MgATP-G-actin after 3 min (*trace 2*) or 4 h (*trace 3*) of incubation at 25°C with EGTA/$MgCl_2$; curve 4 was recorded after 4 h at 25°C and an additional 16 h at 0°C. λ_{ex} = 344 nm.

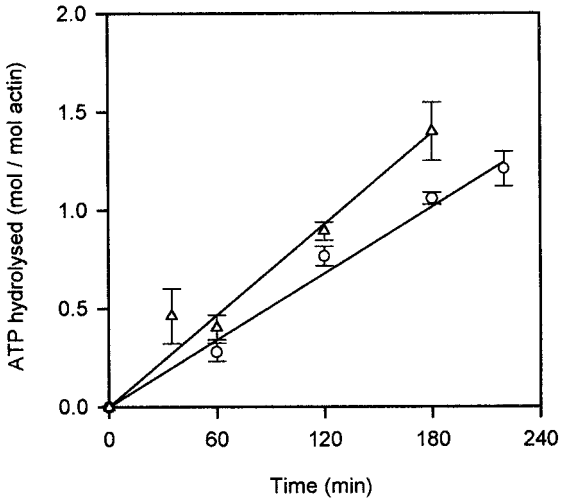

FIGURE 2 ATP hydrolysis in solutions of DED-labeled and unlabeled MgATP-G-actins. Unlabeled (5 μM) (○) and 66% DED-labeled (△) CaATP-G-actin (in 2 mM HEPES, pH 7.6, 30 μM ATP, 50 μM $CaCl_2$, 0.4 mM DTT, and 0.1% NaN_3) was incubated at 25°C with 0.2 mM EGTA/50 μM $MgCl_2$ added at time zero. At intervals, aliquots were taken for determination of inorganic phosphate as described in Materials and Methods. Bars are standard deviation of the measurements from three labeled and four unlabeled actin preparations.

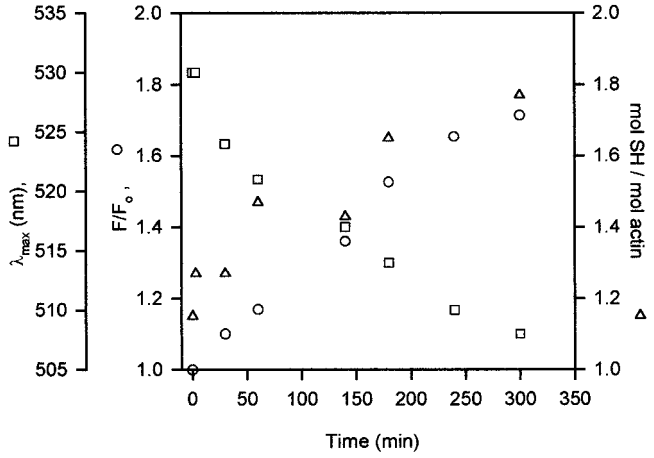

FIGURE 3 Time-dependent changes in the fluorescence emission spectra, and reactivity of the thiol groups of DED-labeled MgATP-G-actin. CaATP-G-actin (3 μM) (73% DED-labeled, in 2 mM HEPES, pH 7.6, 0.2 mM ATP, 50 μM $CaCl_2$, and 0.1% NaN_3) was converted into MgATP-G-actin by the addition of 0.2 mM EGTA/50 μM $MgCl_2$ (time zero in the figure) and left standing in the fluorescence cuvette at 25°C. At time intervals the fluorescence emission spectra were recorded after excitation at 344 nm. From a parallel sample incubated under identical conditions, aliquots were taken for determination of the number of reactive thiol groups. □, Position of λ_{max}; ○, increase in the fluorescence intensity at λ_{max}; △, number of titratable thiol groups.

intramolecular effect of the labeling, or it may be connected to a stimulation of a reversible oligomer formation known to take place in Mg-G-actin solutions (Attri et al., 1991, and references therein). This latter effect may be anticipated in view of the reported stimulation of actin polymerization by DC labeling (Takashi, 1988). A characteristic feature of MgADP-G-actin is an exposure of a second cysteine residue, Cys^{10}, in addition to Cys^{374} carrying the only thiol group easily accessible in ATP-G-actin (Drewes and Faulstich, 1991). In Fig. 3 it is shown that the increase in the fluorescence intensity and blue shift of λ_{max} after the exchange of the bound Ca^{2+} for Mg^{2+} in DED-labeled ATP-G-actin are accompanied by an increase in the number of titratable thiols. On average, ~0.5 mol SH group per mole of actin became exposed within a 3-h incubation of 3 μM MgATP-G-actin, 73–81% DED-labeled, at 25°C (data from four experiments). A transformation of as much as 50% of MgATP-G-actin into the ADP form under these experimental conditions is unlikely, because from the rate of the Mg-G-actin ATPase we can expect hydrolysis of only a small fraction of total ATP (~7.5 μM of 200 μM), and ADP is bound to G-actin (in both Ca- and Mg-bound forms) less tightly than ATP (Kinosian et al., 1993). Thus the instability of the emission spectra of DED- or DC-labeled MgATP-G-actin and the exposure of the cysteine residues of these actins must be related to some other process triggerred by the cation replacement.

The increase in the number of titratable thiols might also be an indication of actin denaturation, which is known to result in an exposure of all four SH groups that are buried in ATP-G-actin (Faulstich et al., 1984; Konno and Morales, 1985; and references therein). In the experiment illustrated in Fig. 4, possible contribution of actin denaturation to the fluorescence changes after replacement of the bound Ca^{2+} with Mg^{2+} was estimated by polymerization of DC-labeled MgATP-G-actin after a 1-h incubation at 25°C, removal of

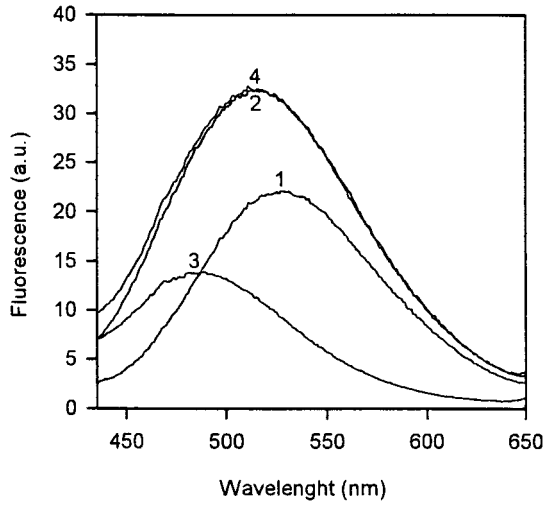

FIGURE 4 Contribution of actin denaturation to the time-dependent changes in the fluorescence emission spectra of DC-labeled MgATP-G-actin. MgATP-G-actin (3 μM) (79% DC-labeled, other conditions as in Fig. 3) was incubated for 1 h at 25°C and then polymerized with 0.1 M KCl and phalloidin at twice actin concentration, and F-actin was sedimented by 30 min of centrifugation at 300,000 × *g*. Traces 1–3 are the fluorescence emission spectra of the initial MgATP-G-actin (*trace 1*), of the same solution after 1 h of incubation at 25°C (*trace 2*), and of the supernatant after sedimentation of polymerized actin (*trace 3*). Trace 4 is a sum of spectra 1 and 3. λ_{ex} = 332 nm.

the polymer by ultracentrifugation, and measurement of the fluorescence spectrum of the protein that remained in the supernatant. Complete transformation of the native G-actin into the polymer was ensured by adding phalloidin at twice the actin concentration, together with salt (Estes et al., 1981; Coluccio and Tilney, 1984). As can be seen, the whole increase in the fluorescence intensity and blue shift of λ_{max} that occurred during the incubation of G-actin in the MgATP form can be accounted for by the fluorescence of the unpolymerized, inactive protein recovered in the supernatant (less than 4% of total actin). To better evaluate the contribution of various steps of actin denaturation to the time-dependent changes in the fluorescence of the labeled MgATP-G-actin, in the subsequent experiments we have examined the changes in the emission spectra accompanying denaturation of actin induced by a removal of the bound cation with EDTA.

Changes in the fluorescence emission spectrum of DC-labeled G-actin upon removal of its bound Ca^{2+} with EDTA. Destabilization of nucleotide-actin complex by labeling of Gln^{41}

Removal of G-actin-bound divalent cation by treatment with metal chelators lowers the affinity of actin to nucleotide (West, 1971; Nowak et al., 1988; Valentin-Ranc and Carlier, 1991; Kinosian et al., 1993) and eventually leads to irreversible inactivation of the nucleotide-free protein (Martonosi and Gouvea, 1961; Bárány et al., 1962; Nagy and Jencks, 1962). Fig. 5 *A* shows changes in the fluorescence emission spectra of DC-labeled CaATP-G-actin developing on the addition of 0.5 mM EDTA at 25°C. An increase in quantum yield of the fluorescence of about sixfold and a shift of the fluorescence maximum from 530 nm ± 2 nm to 491 nm ± 2 nm (average values ± SD from 30 measurements on freshly obtained CaATP-G-actin preparations) were observed. The time courses of these changes, shown in Fig. 5 *B*, could be fitted by a single exponential term with rate constants of $1.1 \pm 0.3 \times 10^{-3}\ s^{-1}$ and $5.7 \pm 0.9 \times 10^{-3}\ s^{-1}$ (mean values ± SD from five measurements) for the fluorescence increase and the shift in position of λ_{max}, respectively. These values are one to two orders of magnitude lower than those reported for the apparent rate constant of Ca^{2+} dissociation from CaATP-G-actin under similar conditions (EDTA or EGTA in large excess over actin, pH in the range 7–8, 20–22°C) (Nowak et al., 1988; Valentin-Ranc and Carlier, 1991). This comparison suggests that the changes in the fluorescence of the dansyl fluorophore are linked to either denaturation or the denaturation-driven dissociation of ATP from cation-free actin rather than to EDTA-induced Ca^{2+} release from the initial CaATP-G-actin complex.

Fig. 5 *B* also shows that the changes in the fluorescence of DC label are accompanied by uncovering of three of the four cysteine residues of actin that are inaccessible to thiol reagents in ATP-G-actin. The apparent first-order rate constant for this process, $6.5 \pm 1.0 \times 10^{-4}\ s^{-1}$ (mean value ± SD from three experiments), was close to that for the increase in the fluorescence intensity. Earlier studies showed that actin with four thiol groups exposed, obtained

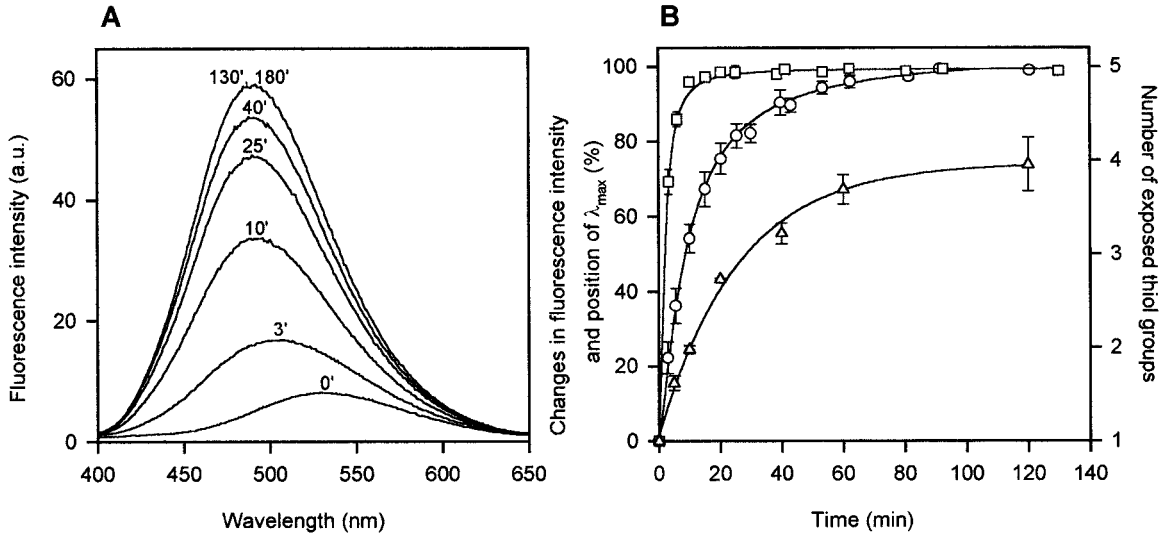

FIGURE 5 Changes in the fluorescence emission spectra and reactivity of the thiol groups of DC-labeled CaATP-G-actin after removal of the bound Ca^{2+} by EDTA. CaATP-G-actin (3 μM) (52% DC-labeled) was supplemented with 0.5 mM EDTA at time 0. At intervals, the fluorescence emission spectra were recorded at 25°C after excitation at 332 nm. From a parallel sample incubated under identical conditions, aliquots were taken at intervals for determination of the number of reactive thiol groups, as described in Materials and Methods. (*A*) Fluorescence emission spectra before and after incubation with EDTA for the times (min) indicated. (*B*) Time courses of changes in relative quantum yield (○) and position of λ_{max} (□) of DC fluorescence (*left ordinate*), and in the number of titratable thiol groups (△, *right ordinate*). The changes in the fluorescence are expressed as a percentage of the final change. The solid curves are the fits to one exponential term; rate constants are given in the text. Bars are the standard deviation of three (△) or five (○, □) measurements; bars are omitted if the range is smaller than the symbol.

by a fast depolymerization of F-actin in ATP-free buffer solution, loses its polymerizability (at 4°C) in only ~30 min (Faulstich et al., 1984). This confirms that the EDTA-induced thiol group exposure and the accompanying enhancement of the fluorescence of DC-labeled actin monitor accumulation of an intermediate of actin denaturation.

To verify that the changes in the fluorescence of DC label are linked to the time-dependent loss of the bound nucleotide from metal ion-free actin, we measured the rate of the fluorescence increase in the presence of EDTA as a function of ATP concentration. Because ATP is in rapid equilibrium with cation-free actin, and nucleotide-free actin irreversibly denatures, the experimental rate constants (k_{exp}) for the increase in DC fluorescence taken as a measure of the denaturation should show the following dependence on ATP concentration (Nowak et al., 1988; Kinosian et al., 1993):

$$1/k_{exp} = 1/k_d + [ATP]/k_d K_{diss}) \quad (1)$$

where k_d is the first-order rate constant of denaturation and K_{diss} is the equilibrium dissociation constant of ATP from cation-free actin. Fig. 6 shows that, indeed, the reciprocal of the observed rate constant for the fluorescence change is a linear function of ATP concentration at least up to 100 μM. Linear regression yielded values of $k_d = 1.0 \pm 0.2 \times 10^{-2}$ s^{-1} and $K_{diss} = 4.0 \pm 1.3 \times 10^{-5}$ M.

Our observation that the thiol group exposure in EDTA-treated actin parallels the release of nucleotide rather than the removal of cation is in disagreement with earlier studies

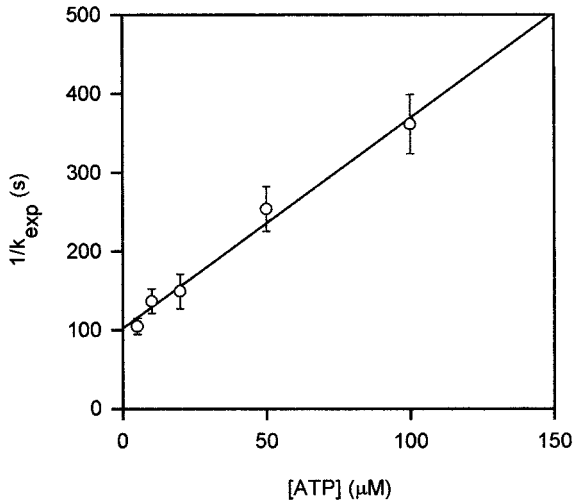

FIGURE 6 Dependence of the rate of EDTA-induced change in the fluorescence intensity of DC-labeled G-actin on ATP concentration. Samples of 2 μM CaATP-G-actin (78–84% DC-labeled) in 2 mM HEPES (pH 7.6), 10 μM $CaCl_2$, 0.2 mM DTT, and various concentrations of ATP were supplemented with 1 mM EDTA, and the changes in DC fluorescence were recorded at 491 nm (λ_{max} for denatured actin) after excitation at 332 nm, at 25°C. The reciprocals of the rate of increase in the fluorescence intensity are plotted versus ATP concentration. The mean values and the linear regression line for data points from four independent experiments are shown. Bars are the standard deviation of the mean.

indicating an exposure from two to four cysteine residues in cation-free ATP-G-actin (Konno and Morales, 1985; Valentin-Ranc and Carlier, 1991). This discrepancy seems to be due to the use in these earlier works of a slowly reacting thiol reagent, 5,5′-dithiobis(2-nitrobenzoic acid) (DTNB), and, consequently, much longer incubation of EDTA-treated actin with the reagent than is required for the reaction with HEDD used here. In our experience, the joint presence of EDTA and a thiol reagent largely accelerates the exposure of actin thiol groups.

From the results described in this and in the preceding section, it is clear that the presence of even small amounts of denatured protein in actin preparations has a large impact on the fluorescence emission spectra of dansyl fluorophores on Gln^{41}. Indeed, we have noticed a gradual blue shift of the emission spectra of both DC- and DED-labeled G-actin left standing on ice, even if it was in the most stable CaATP form. Removal of denatured actin by a polymerization-ultracentrifugation-depolymerization cycle restored the original spectra of freshly prepared CaATP-G-actin. The large acceleration of denaturation of the labeled actin by replacement of the bound Ca^{2+} with Mg^{2+}, which appears to be responsible for the increased instability of the fluorescence spectra of MgATP-G-actin, seems to be underlain by two effects of the bound Mg^{2+}. The stimulation of the G-actin ATPase may lead to a depletion of free ATP and conversion of MgATP-G-actin into the unstable MgADP form when this actin is stored at high protein concentrations. At 0°C, 85% DED-labeled MgATP-G-actin hydrolyzed nearly 3 mol ATP/mol actin within 22 h. One can calculate that 50 μM actin would consume all free ATP (usually 200 μM) within ~29 h. The other effect of Mg^{2+} is related to the lower rate constant of reassociation of this cation with actin relative to Ca^{2+}. Replacement of Ca^{2+} with Mg^{2+} accelerates actin denaturation because the average time that actin spends cation free, with a reduced affinity for nucleotide, is longer for Mg-G-actin than for Ca-G-actin, and nucleotide-free actin undergoes a fast denaturation (Kinosian et al., 1993, and references therein). Conversion of MgATP-G-actin into the less stable MgADP form (Gershman et al., 1989) increases the probability of nucleotide (ADP) dissociation from the monomers that are momentarily free of the bound divalent cation and of denaturation of the nucleotide-free monomers before the rebinding of ATP present in the solution and stabilization of the nucleotide-actin complex by rebinding of Mg^{2+}. In view of the decreased affinity of the labeled actin for nucleotide, this effect seems to explain the relatively fast denaturation of the MgATP form of this actin, even at low protein concentrations at which no significant accumulation of MgADP-G-actin can be expected on the time scale of our experiments.

Effects of ATP/ADP exchange at the nucleotide site on the environment of Gln^{41} in G-actin

The instability of ADP-G-actin and the large changes in the environment of dansyl fluorophores on Gln^{41} shown here to

accompany denaturation of the labeled protein call for caution in the interpretation of the fluorescence changes observed upon conversion of ATP-G-actin into ADP-G-actin. Incubation of MgATP-G-actin with hexokinase and glucose to transform free ATP into ADP, which then exchanges with the bound ATP, was shown to be the fastest and most efficient procedure of preparing G-actin with ADP at the nucleotide site (Gershman et al., 1989). However, even this procedure does not seem to avoid some denaturation of labeled actin before the exchange comes to completion. As can be seen in Fig. 7, the time course of changes in the fluorescence of DC-labeled MgATP-G-actin after the addition of hexokinase was clearly biphasic. The initial, faster phase lasted for 60–100 min, a period sufficient to convert unlabeled MgATP-G-actin into MgADP-G-actin under conditions used in these experiments, and resulted in an enhancement of the fluorescence quantum yield of about twofold and in a shift of the fluorescence maximum from 531 nm to 520–522 nm. No stable fluorescence plateau was established, however. An increase in the quantum yield of about fourfold and a shift of the fluorescence maximum to 489 nm observed after a 24-h incubation at 0°C show that the spectra registered after prolonged incubation of the labeled actin in MgADP form, even at high (1 mM) free ADP concentration, are dominated by changes characteristic of denatured actin. This is also apparent from the incomplete reversibility of the fluorescence change upon the addition of excess ATP to replace the bound ADP after various incubation times. As can be seen in Fig. 7 *A*, initially the reversibility increased with time, reflecting an increase of the fraction of actin that had been converted into the ADP form before the addition of ATP. However, even in this initial phase, only ~50% of the fluorescence change (after a 60-min incubation with hexokinase and glucose) could be reversed by adding ATP in a fourfold molar excess over ADP. In the second phase of the changes, the reversibility gradually diminished, down to 12–14% after 24 h. Although incomplete reconversion of the ADP-actin into ATP-actin might have made some contribution to the irreversible part of the fluorescence change, as Mg-G-actin binds ATP with an affinity only about fourfold higher than that for ADP (Kinosian et al., 1993), the experiments described below confirm that it is mostly related to fast denaturation of the labeled MgADP-G-actin.

Fig. 8 shows representative results of experiments in which, after exchange of ATP for ADP, nondenatured actin was polymerized in the presence of phalloidin to lower the critical concentration for polymerization, and the emission spectrum of supernatant after removal of the polymer by ultracentrifugation (*trace 4*) was compared with those of MgATP-G-actin (*trace 1*) and the MgADP-G-actin solution (*trace 2*). From these data and from the amount of actin remaining in the supernatant, one can calculate the spectrum resulting from the replacement of bound ATP with ADP in native actin (*trace 5*). In agreement with the magnitude of the reversible part of the fluorescence change by the end of

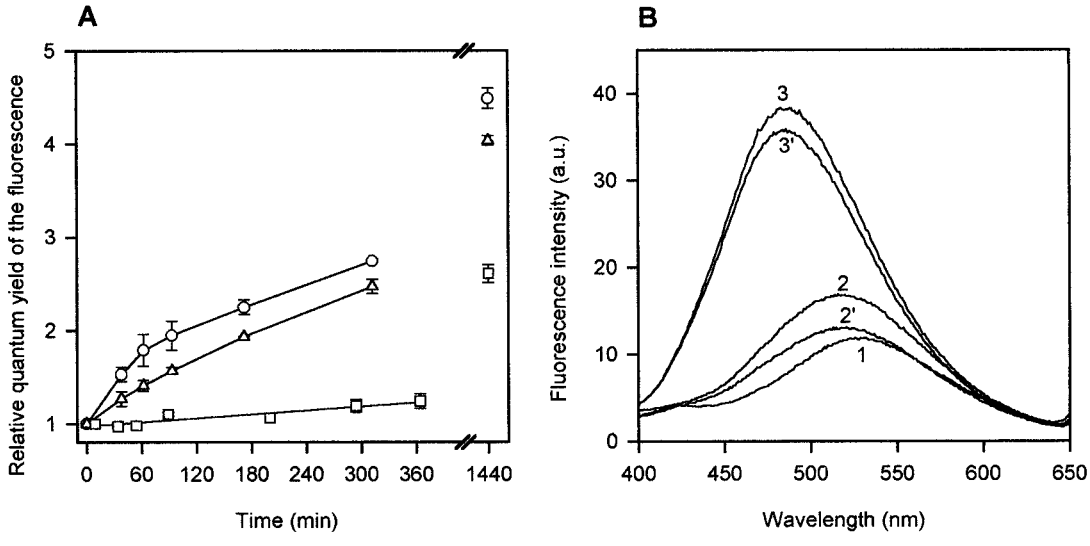

FIGURE 7 Changes in the fluorescence emission spectra of DC label accompanying a conversion of the labeled MgATP-G-actin into MgADP-G-actin. CaATP-G-actin (5 μM) (70–87% DC-labeled, in 2 mM HEPES (pH 7.6), 0.2 mM ATP, 0.05 mM $CaCl_2$, 0.2 mM DTT, 0.3 mM glucose, and 0.1% NaN_3) was incubated with 0.2 mM EGTA and 50 μM $MgCl_2$ for 8 min at 0°C to replace bound Ca^{2+} with Mg^{2+}. Then (time 0 in the figure) 0.8 mM ADP and hexokinase (20 U/ml) were added. After various times, aliquots of the solution (kept at 0°C) were diluted fivefold with a buffer solution containing 2 mM HEPES (pH 7.6), 0.2 mM EGTA, and 50 μM $MgCl_2$, and the fluorescence emission spectra were recorded at 5°C after excitation at 332 nm. Immediately after that, ATP at a final concentration of 1 mM was added to each sample to replace the bound ADP with ATP. The exchange reaction was monitored by measuring the decrease in the fluorescence intensity, and then the final spectra were recorded. (*A*) Relative quantum yield of DC fluorescence before (○) and after exchange of bound ADP for ATP (△). The quantum yield of MgATP-G-actin at time 0 was taken as 1. Time-dependent changes in the fluorescence of MgATP-G-actin (□) are also shown. Bars are the range of data points from two experiments; bars are omitted if the range is smaller than the symbol. The curves were drawn through data points. (*B*) Fluorescence emission spectra before (*traces 1, 2,* and *3*), and after exchange of ATP into actin (*traces 2′* and *3′*) at time 0 (*trace 1*), 62 min (*traces 2* and *2′*), and 24 h (*traces 3* and *3′*). All data are corrected for dilutions.

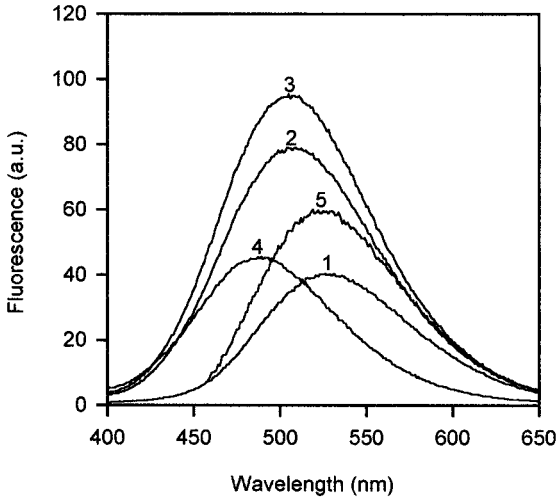

FIGURE 8 Changes in the fluorescence emission spectrum of DC-labeled Mg-G-actin directly linked to a replacement of the bound ATP with ADP. MgATP-G-actin (5 μM) (80% DC-labeled) was incubated with hexokinase and glucose as described in the legend to Fig. 7, at 5°C for 2.5 h to ensure a complete conversion into MgADP-G-actin. Actin was then polymerized with 0.1 M KCl and phalloidin at twice the actin concentration, and F-actin was sedimented by a 30-min centrifugation at 300,000 × *g*. Traces 1–4 are the fluorescence emission spectra of the initial MgATP-G-actin (*trace 1*), of the same solution after the incubation with hexokinase and glucose (*trace 2*) and after subsequent polymerization (*trace 3*), and of the supernatant after sedimentation of the polymer (*trace 4*). Trace 5 is the spectrum of 5 μM MgADP-G-actin, obtained as the difference between spectra 2 and 4 multiplied by a factor of $c_t/(c_t - c_s)$, where c_t and c_s are the protein concentrations of total actin and of that in the supernatant, respectively. The directly measured spectra are corrected for dilutions.

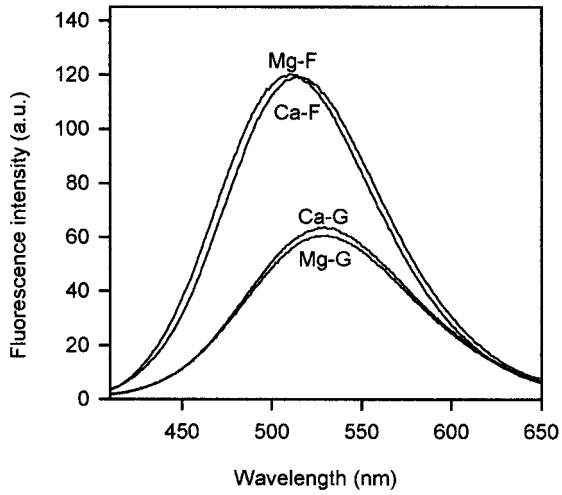

FIGURE 9 Polymerization-induced changes in the fluorescence emission spectra of DC-labeled CaATP-G-actin and MgATP-G-actin. CaATP-G-actin (5 μM) (90% DC-labeled) was polymerized with 0.1 M KCl directly (Ca-actin) and, in a parallel sample, after a 3-min incubation with 0.2 mM EGTA and 50 μM $MgCl_2$ (Mg-actin). Emission spectra of the G-actins (Ca-G, Mg-G) and F-actins (Ca-F, Mg-F) were recorded at 25°C, after excitation at 332 nm.

the exchange reaction, an increase in the fluorescence intensity of ~40% and a 4-nm blue shift of λ_{max} were found to be directly linked to the nucleotide exchange. These changes, suggesting a transfer of the probe to a more hydrophobic environment, are still large and confirm the conclusion that conversion of MgATP-G-actin into MgADP-G-actin results in a profound change in the conformation of the loop 38–52.

Effects of polymerization on the environment of Gln^{41} in actin

Earlier examination of polymerization-related changes in the environment of Gln^{41} with DED- or DC-labeled actins suggested a very small change in MgATP-G-actin (polymerized with $MgCl_2$) in contrast to a large change in CaATP-G-actin polymerized with either $CaCl_2$ (Kim et al., 1995) or $MgCl_2$ (Takashi, 1988). Our comparison of polymerization effects on the fluorescence spectra of both DC- and DED-labeled MgATP- and CaATP-actins showed no significant cation-dependent difference, provided that polymerization of MgATP-G-actin was started shortly after replacement of the bound Ca^{2+} with Mg^{2+}. An increase in the fluorescence intensity of more than twofold and a 10–16-nm blue shift in λ_{max} was observed with both 0.1 M KCl as the polymerizing salt (Fig. 9, Table 1) and with 2 mM $CaCl_2$ used for CaATP-G-actin and 2 mM $MgCl_2$ for MgATP-G-actin (data not shown). The failure to observe a similar change in MgATP-G-actin in the earlier study might have been due to a prolonged storage of this actin before polymerization, which, as was shown here, results in spectral changes that may overshadow the polymerization-dependent change. A time-dependent decrease in the concentration of polymerizable actin, due to the Mg^{2+}-stimulated ATP hydrolysis, converting ATP-G-actin into ADP-G-actin (which has a higher critical concentration for polymerization; Gershman et al., 1989), and to partial denaturation of the unstable MgATP form and, in particular, the MgADP form, can also be expected. This explanation is consistent with the results in Fig. 10 showing that storage of 3 μM MgATP-G-actin at 0°C reduced the polymerization-induced increase in DED fluorescence from a 2.3-fold to 1.9- and 1.6-fold after 24 and 48 h, respectively, mostly because of an increase in the fluorescence of the initial MgATP-G-actin. Fig. 10 also shows a time-dependent change in the kinetics of polymerization upon storage of G-actin in the Mg^{2+}-bound form: the disappearance of the initial lag phase is an indication of a Mg^{2+}-dependent oligomerization (Newman et al., 1985), which itself may have made some contribution to the fluorescence enhancement in G-actin and may accelerate the hydrolysis of ATP in this actin, as discussed in one of the preceding sections.

Because the polymerization-dependent changes in the emission spectra of DC- and DED-labeled actins are qualitatively similar to the changes observed upon substitution of ADP for ATP in G-actin, it is reasonable to suppose that they are related at least in part to the changes in the conformation of loop 38–52 suggested to occur upon the release of P_i from F-ADP-P_i intermediate generated by ATP

TABLE 1 Summary of the effects of Ca^{2+} with Mg^{2+} and ATP with ADP replacements in G-actin, and of KCl-induced polymerization of CaATP-G-actin or MgATP-G-actin, on the fluorescence of DC or DED label

	DC-actin		DED-actin	
Actin species	λ_{max} (nm)	Q/Q_0	λ_{max} (nm)	Q/Q_0
CaATP-G-actin	530 ± 2 (25)		535 ± 1 (14)	
MgATP-G-actin	528 ± 3 (13)	0.97 ± 0.05 (10)	535 ± 1 (5)	0.97 ± 0.05 (21)
MgADP-G-actin	524 ± 1 (3)	1.4 ± 0.06 (3)		
Ca-F-actin	516 ± 1 (8)	2.24 ± 0.31 (8)	525 ± 1 (5)	2.37 ± 0.03 (5)
Mg-F-actin	512 ± 3 (8)	2.13 ± 0.39 (8)	526 ± 1 (4)	2.81 ± 0.13 (4)

The data are means ± SEM from the number of determinations given in parentheses. Q/Q_0 is the relative quantum yield of the fluorescence, obtained from the area under the peak, with the quantum yield of the initial form of actin (i.e., CaATP-G form for MgATP-G-actin, MgATP-G form for MgADP-G-actin, and CaATP-G-actin or MgATP-G-actin for Ca- and Mg-F-actin, respectively) taken as 1.

hydrolysis during polymerization (Orlova and Egelman, 1992; Muhlrad et al., 1994). This conclusion is supported by comparison of time courses of polymer formation, monitored by measuring an increase in the light scattering intensity, and the increase in the fluorescence intensity after the addition of polymerizing salt. When the scatter of the results was eliminated by carrying out both measurements alternately on the same protein sample, it was reproducibly observed that the fluorescence change accompanying polymerization of Ca-G-actin lagged slightly behind the polymer formation (Fig. 11 *A*), whereas in Mg-G-actin these changes proceeded at virtually the same rates (Fig. 11 *B*). These relationships seem to reflect the lagging of ATP hydrolysis and of the subsequent release of inorganic phosphate behind polymerization, which is easily seen with CaATP-actin but is not detectable with MgATP-actin under conditions of the relatively slow spontaneous polymerization (Carlier and Pantaloni, 1986; Carlier et al., 1987).

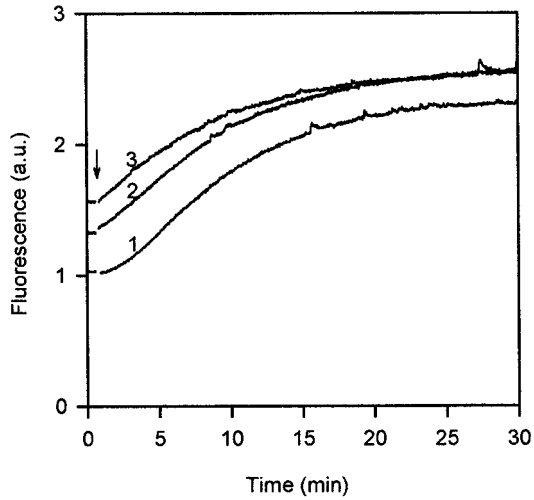

FIGURE 10 Effects of storage of MgATP-G-actin on the polymerization-induced changes in the fluorescence of DED label. MgATP-G-actin (3 μM) (74% DED-labeled, in 2 mM HEPES (pH 7.6), 0.2 mM ATP, 50 μM $MgCl_2$, 0.2 mM EGTA, 0.2 mM DTT, and 0.01% NaN_3) was polymerized with 0.1 M KCl immediately after replacement of the initially bound Ca^{2+} with Mg^{2+} (*trace 1*) or after storage for 24 h (*trace 2*) or 48 h at 0°C (*trace 3*). The changes in the fluorescence intensity at 525 nm after the addition of KCl (*arrow*) were recorded at 25°C. λ_{ex} = 344 nm.

Another type of evidence in support of the contribution of the nucleotide-dependent conformational change to the change accompanying polymerization comes from an examination of the effects of beryllium fluoride (BeF_x) on the

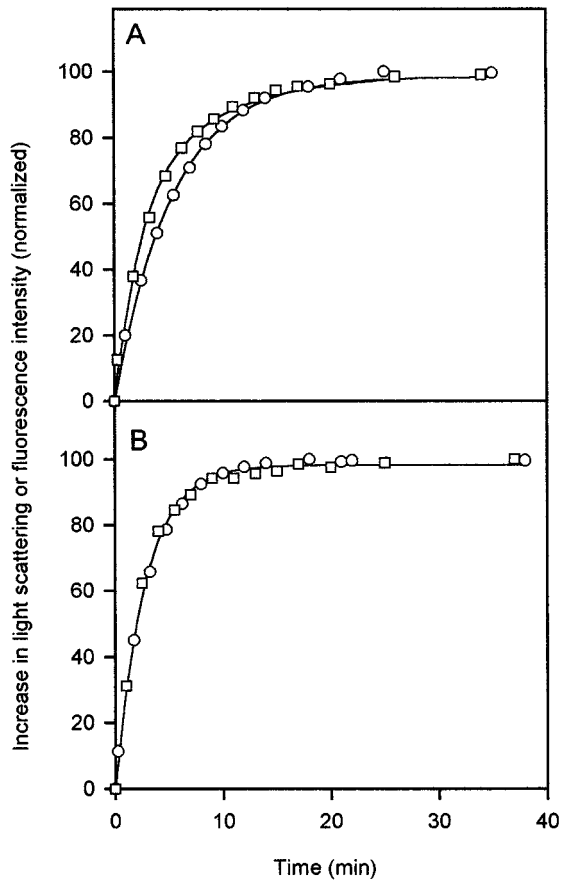

FIGURE 11 Time courses of polymerization and of the accompanying increase in the fluorescence intensity of DC-labeled CaATP-G-actin and MgATP-G-actin. CaATP-G-actin (10 μM) (*A*) and 5 μM MgATP-G-actin (*B*), 73% DC-labeled, were polymerized with 0.1 M KCl at 25°C. At intervals, light-scattering intensity at 450 nm (□) and fluorescence intensity at 512 nm (○) were alternately measured. The light-scattering and fluorescence intensities at time 0 and at steady state were normalized to 0 and to 100, respectively. The smooth curves were drawn through the data points. The Mg-G-actin was obtained by a 3-min incubation of Ca-G-actin with 0.2 mM EGTA/50 μM $MgCl_2$ at 25°C.

emission spectrum of DC-F-actin. As can be seen in Fig. 12, the slow binding of BeF_x, producing an analog of the transient state F-ADP-P_i in actin polymerization (Combeau and Carlier, 1988), resulted in a reversal of a significant part (on the average, 25 ± 4%) of the change in DC fluorescence intensity that had occurred during polymerization of MgATP-G-actin and in a 4-nm red shift of λ_{max}. Interestingly, the magnitude of this reversible part of the polymerization-induced change in the fluorescence intensity relative to the fluorescence intensity of the initial MgATP-G-actin (~36%) is close to the magnitude of the fluorescence change produced by ATP for ADP exchange in G-actin. Of the same magnitude in both cases are the shifts in λ_{max}.

DISCUSSION

The results of this work clearly show that replacement of Ca^{2+} with Mg^{2+} at the single high-affinity site for divalent cation in G-actin is accompanied by a small quenching of the fluorescence of both DC- and DED-labeled actin, and that the previously reported increase in the fluorescence intensity and blue shift of λ_{max} (Kim et al., 1995; Moraczewska et al., 1996) must have reflected slow conformational transition(s) subsequent to the conversion of CaATP-G-actin into MgATP-G-actin. An increase in the fluorescence intensity and blue shift of λ_{max}, albeit much slower, were also observed during storage of G-actin in the CaATP form. Their acceleration by replacement of the bound Ca^{2+} with Mg^{2+} seems to result from concerted effects of the slow hydrolysis of ATP on Mg-G-actin, converting MgATP-G-actin into the less stable MgADP form, and of denaturation-driven dissociation of the bound nucleotide, leading to large changes in the fluorescence emission spectra. Slow transformation of G-actin preparations stored in the MgATP form into MgADP-G-actin and partial denaturation of actin might also underlie the inhibition of subtilisin cleavage at Met^{47} suggested to result from substitution of Mg^{2+} for Ca^{2+} (Kim et al. 1995), as this inhibition is a characterisic feature of both MgADP-G-actin and of a transient state of EDTA-induced G-actin denaturation (Hozumi, 1988; Strzelecka-Gołaszewska et al., 1993; Muhlrad et al., 1994), and it was not observed with actin digested immediately after the exchange of Ca^{2+} for Mg^{2+} (Strzelecka-Gołaszewska et al., 1993).

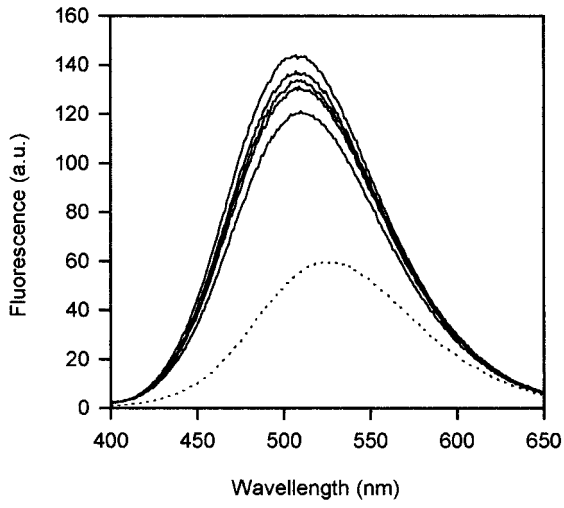

FIGURE 12 Effects of BeF_x on the fluorescence emission spectrum of DC-labeled F-actin. MgATP-G-actin (10 μM) (58% DC-labeled, in 2 mM HEPES (pH 7.6), 0.2 mM ATP, 50 μM $MgCl_2$, 0.2 mM EGTA, 0.2 mM DTT, and 0.01% NaN_3) was polymerized with 2 mM $MgCl_2$ and then supplemented with equimolar $BeS0_4$ and NaF in a 50-fold molar excess. Solid traces, from top to bottom, are the emission spectra of the F-actin alone, and after 1, 2, 3, and 24 h of incubation with BeF_x at 25°C, respectively. The dotted trace is the spectrum of the initial MgATP-G-actin. λ_{ex} = 332 nm.

The contribution of nucleotide dissociation to the instability of the fluorescence spectra of DC- or DED-labeled G-actin is substantiated by the character, magnitude, and dependence of the rates of the fluorescence changes after the removal of bound Ca^{2+} from CaATP-G-actin with EDTA on free ATP concentration. The equilibrium constant for dissociation of ATP from cation-free DC-actin derived from these measurements, $K_{diss} = 4 \times 10^{-5}$ M at 25°C, pH 7.6, is an order of magnitude higher than the K_{diss} values obtained from the rates of changes in tryptophan fluorescence of unmodified actin (Kinosian et al., 1993; Ooi and Mihashi, 1996), but similar to (or lower than) those derived from the rates of a decrease in the fluorescence of 5-{2-[amino]ethyl}aminonaphthalene-1-sulfonic acid-actin (AEDANS-actin) (Nowak et al., 1988; Valentin-Ranc and Carlier, 1991). This comparison suggests that labeling of Gln^{41} with dansyl fluorophores, as well as AEDANS labeling of Cys^{374}, diminishes the affinity of actin for nucleotide. This effect of labeling might explain the wide scatter of the reported values of K_{diss} for ATP binding to cation-free actin obtained using the same procedure but different signals of the protein denaturation, and it seems to be crucial for the destabilization of G-actin by DC or DED labeling. A similar consequence of subtilisin cleavage of actin at Met^{47}, a few residues from the attachment site for the dansyl probes, has recently been described (Ooi and Mihashi, 1996). Destabilization of actin by its labeling at Cys^{374} with erythrosin-5-iodoacetamide has also been reported (Ludescher and Liu, 1993). These effects are consistent with and confirm the structural coupling between the nucleotide site, subdomain 2, and the C-terminus in G-actin (Frieden and Patane, 1985; Strzelecka-Gołaszewska et al., 1993, 1995; Muhlrad et al., 1994; Crosbie et al., 1994; Kuznetsova et al., 1996). The sensitivity of the environment Gln^{41} to ATP/ADP exchange and acceleration of ATP hydrolysis on MgATP-G-actin by labeling of this residue are other signs of the structural relationship between the nucleotide site and loop 38–52.

The results of this work show that fluorescence spectroscopy of actin labeled with dansyl probes covalently attached to Gln^{41} is a powerful technique for the study of physiological changes in the environment of this residue, provided that the diminished stability of the labeled protein and its consequences are taken into account. In particular, storage of labeled G-actin with Mg^{2+} bound at the high-affinity site

should be avoided. The effect of Ca^{2+}/Mg^{2+} exchange on the environment of Gln^{41} can easily be evaluated using the fast cation exchange procedure in which formation of MgATP-G-actin is facilitated by chelation of free Ca^{2+} with EGTA (Gershman et al., 1986). Evaluation of the effect of ATP for ADP exchange in G-actin requires correction for protein denaturation resulting from the instability of the ADP form.

Our present finding that the change in the environment of Gln^{41} accompanying replacement of the bound Ca^{2+} with Mg^{2+} is not only quantitatively but also qualitatively different from changes associated with conversion of ATP-G-actin into ADP-G-actin (Table 1) supports the suggestion (Moraczewska et al., 1996) that these effects reflect entirely different structural transitions in G-actin. Narrowing of the interdomain cleft by a shift of subdomains 2 and 4 closer together upon replacement of Ca^{2+} by Mg^{2+} in ATP-G-actin, proposed to explain the suppression of proteolytic cleavages at sites facing the cleft (Strzelecka-Gołaszewska et al., 1996), has been confirmed by molecular dynamics simulations (Wriggers and Schulten, 1996). The relatively small change in the fluorescence of probes on Gln^{41} as well as the earlier documented insensitivity of proteolytic cleavage sites within the DNase I–binding loop to Ca^{2+}/Mg^{2+} replacement in G-actin (Strzelecka-Gołaszewska et al., 1993) suggest that the stabilization by Mg^{2+} of the "closed conformation" of the monomer is not associated with any substantial change in the structure of loop 38–52 on the top of subdomain 2. The results presented here also show that in F-actin subunits too the environment of Gln^{41} is not significantly influenced by the type of tightly bound cation, which seems to preclude a substantial cation-dependent change in the monomer-monomer contacts involving this segment of the loop. In contrast, the effects of substitution of ADP for ATP in G-actin seem to involve a profound change in this area of the molecule. The increase in the fluorescence intensity and blue shift of the emission spectra of dansyl probes on Gln^{41} (Kim et al., 1995; Moraczewska et al., 1996, and this work) and the diminished proteolytic susceptibility of loop 38–52 in ADP-G-actin (Strzelecka-Gołaszewska et al., 1993; Muhlrad et al., 1994) indicate that this loop, which in ATP-G-actin is disordered and highly mobile (McLoughlin et al., 1993), assumes a more compact structure after replacement of the bound ATP with ADP. It has been suggested that in MgADP-G-actin this loop folds back onto subdomain 2 (Strzelecka-Gołaszewska et al., 1993; Moraczewska et al., 1996). This idea received a support from crystallographic investigations of β-actin in an "open" and "tight" state, showing that loop 38–52 can indeed change its conformation from an extended one to fold back onto subdomain 2 (Chik et al., 1996; Page et al., 1998).

The increase in hydrophobicity of the environment of Gln^{41} upon polymerization of actin, apparent from the increase in quantum yield and blue shift of the emission spectra of dansyl probes, is consistent with the suggested participation of loop 38–52 in hydrophobic monomer-monomer contacts (Holmes et al., 1990; Lorenz et al., 1993; Tirion et al., 1995). However, a significant part of this change appears to be linked to the rearrangement of loop 38–52 suggested to occur upon ATP hydrolysis and P_i release subsequent to the monomer incorporation into a growing filament (Orlova and Egelman, 1992; Muhlrad et al., 1994). This is indicated by 1) the lagging of the fluorescence increase behind the polymerization in Ca-actin but not in Mg-actin, which correlates with the cation-dependent difference in the extent of the uncoupling of ATP hydrolysis from the polymer formation (Carlier and Pantaloni, 1986; Carlier et al., 1987), and 2) the partial reversibility of the fluorescence changes upon binding of BeF_x, which produces an analog of the transient ADP-P_i-F-actin state (Combeau and Carlier, 1988). The similarity of the character and magnitude of the reversible part of the polymerization-induced fluorescence changes to those resulting from replacement of ATP with ADP in G-actin supports the suggestion (Strzelecka-Gołaszewska et al., 1993; Moraczewska et al., 1996) that the nucleotide-dependent changes in the conformation of loop 38–52 in G- and F-actin are of similar character and provide a common structural basis for the poor polymerizability of ADP-G-actin and destabilization of the polymer by ATP hydrolysis and P_i release.

At the end, it is worth noting that although the data presented here suggest that the cation-dependent conformational transitions in both G- and F-actin structure do not significantly influence loop 38–52 on the top of subdomain 2, there is an indirect effect of the tightly bound cation on this loop in F-actin, through the acceleration by Mg^{2+} of ATP hydrolysis and P_i release, which convert ATP-F-actin into ADP-F-actin (Carlier et al., 1987; Carlier, 1991). At steady state this effect is obviously limited to the filament ends and, therefore, is undetectable by techniques averaging the signals from all actin protomers.

We thank Prof. Emil Reisler of the Department of Chemistry and Biochemistry, University of California, Los Angeles, for helpful discussions. The excellent technical assistance of Mrs. E. Karczewska is acknowledged.

This work was supported by a grant to the Nencki Institute from the State Committee for Scientific Research.

REFERENCES

Attri, A. K., M. C. Lewis, and E. D. Korn. 1991. The formation of actin oligomers studied by analytical ultracentrifugation. *J. Biol. Chem.* 266: 6815–6824.

Bárány, M., F. Finkelman, and T. Therattil-Antony. 1962. Studies on the bound calcium of actin. *Arch. Biochem. Biophys.* 98:28–45.

Bitny-Szlachto, S. 1960. Reaction of mercaptans with unsymmetrical disulphides. *Acta Pol. Pharm.* 17:373–385.

Carlier, M.-F. 1991. Actin: protein structure and filament dynamics. *J. Biol. Chem.* 266:1–4.

Carlier, M.-F., and D. Pantaloni. 1986. Direct evidence for ADP-P_i-F-actin as the major intermediate in ATP-actin polymerization. Rate of dissociation of P_i from actin filaments. *Biochemistry.* 25:7789–7792.

Carlier, M.-F., D. Pantaloni, and E. D. Korn. 1987. The mechanisms of ATP hydrolysis accompanying the polymerization of Mg-actin and Ca-actin. *J. Biol. Chem.* 262:3052–3059.

Chik, J. K., U. Lindberg, and C. E. Schutt. 1996. The structure of an open state of beta-actin at 2.65 Å resolution. *J. Mol. Biol.* 263:607–623.

Coluccio, L. M., and L. G. Tilney. 1984. Phalloidin enhances actin assembly by preventing monomer dissociation. *J. Cell Biol.* 99:529–535.

Combeau, C., and M.-F. Carlier. 1988. Probing the mechanism of ATP hydrolysis on F-actin using vanadate and the structural analogs of phosphate BeF_3^- and AlF_4^-. *J. Biol. Chem.* 263:17429–17436.

Crosbie, R. H., C. Miller, P. Cheung, T. Goodnight, A. Muhlrad, and E. Reisler. 1994. Structural connectivity in actin: effect of C-terminal modifications on the properties of actin. *Biophys. J.* 67:1957–1964.

Drewes, G., and H. Faulstich. 1991. A reversible conformational transition in muscle actin is caused by nucleotide exchange and uncovers cysteine in position 10. *J. Biol. Chem.* 266:5508–5513.

Eligula, L., L. Chuang, M. L. Phillips, M. Motoki, K. Seguro, and A. Muhlrad. 1998. Transglutaminase-induced cross-linking between subdomain 2 of G-actin and the 636–642 lysine-rich loop of myosin subfragment 1. *Biophys. J.* 74:953–963.

Estes, J. E., L. A. Selden, and L. C. Gershman. 1981. Mechanism of action of phalloidin on the polymerization of muscle actin. *Biochemistry.* 20:708–712.

Estes, J. E., L. A. Selden, and L. C. Gershman. 1987. Tight binding of divalent cations to monomeric actin. Binding kinetics support a simplified model. *J. Biol. Chem.* 262:4952–4957.

Estes, J. E., L. A. Selden, H. J. Kinosian, and L. C. Gershman. 1992. Tightly bound divalent cation of actin. *J. Muscle Res. Cell Motil.* 13:272–284.

Faulstich, H., I. Merkler, H. Blackholm, and C. Stournaras. 1984. Nucleotide in monomeric actin regulates the reactivity of the thiol groups. *Biochemistry.* 23:1608–1612.

Frieden, C., and K. Patane. 1985. Differences in G-actin containing bound ATP or ADP: the Mg^{2+}-induced conformational change requires ATP. *Biochemistry.* 24:4192–4196.

Gershman, L. C., L. A. Selden, and J. E. Estes. 1986. High affinity binding of divalent cation to actin monomer is much stronger than previously reported. *Biochem. Biophys. Res. Commun.* 135:607–614.

Gershman, L. C., L. A. Selden, H. J. Kinosian, and J. E. Estes. 1989. Preparation and polymerization properties of monomeric ADP-actin. *Biochim. Biophys. Acta.* 995:109–115.

Hegyi, G., G. Premecz, B. Sain, and A. Muhlrad. 1974. Selective carboethoxylation of the histidine residues of actin by diethyl pyrocarbonate. *Eur. J. Biochem.* 44:7–12.

Holmes, K. C., D. Popp, W. Gebhard, and W. Kabsch. 1990. Atomic model of actin filament. *Nature.* 347:44–49.

Houk, W. T., and K. Ue. 1974. The measurement of actin concentration in solution: a comparison of methods. *Anal. Biochem.* 62:66–74.

Huang, Y.-P., K. Seguro, M. Motoki, and K. Tawada. 1992. Cross-linking of contractile proteins from skeletal muscle by treatment with microbial transglutaminase. *J. Biochem. (Tokyo).* 112:229–234.

Kabsch, W., H. G. Mannherz, D. Suck, E. F. Pai, and K. Holmes. 1990. Atomic structure of the actin: DNase I complex. *Nature.* 347:37–44.

Khaitlina, S. Y., J. Moraczewska, and H. Strzelecka-Gołaszewska. 1993. The actin/actin interactions involving the N-terminus of the DNase-I-binding loop are crucial for stabilization of the actin filament. *Eur. J. Biochem.* 218:911–920.

Kim, E., M. Motoki, K. Seguro, A. Muhlrad, and E. Reisler. 1995. Conformational changes in subdomain 2 of G-actin: fluorescence probing by dansyl ethylenediamine attached to Gln-41. *Biophys. J.* 69: 2024–2032.

Kinosian, H. J., L. A. Selden, J. E. Estes, and L. C. Gershman. 1993. Nucleotide binding to actin. Cation dependence of nucleotide dissociation and exchange rates. *J. Biol. Chem.* 268:8683–8691.

Kodama, T., K. Fukui, and K. Kometani. 1986. The initial phosphate burst in ATP hydrolysis by myosin and subfragment-1 as studied by a modified malachite green method for determination of inorganic phosphate. *J. Biochem. (Tokyo).* 99:1465–1472.

Konno, K., and M. Morales. 1985. Exposure of actin thiols by the removal of tightly held calcium ions. *Proc. Natl. Acad. Sci. USA.* 82:7904–7908.

Kuznetsova, I., O. Andropova, K. Turoverov, and S. Khaitlina. 1996. Conformational changes in subdomain I of actin induced by proteolytic cleavage within the DNase-I-binding loop: energy transfer from tryptophan to AEDANS. *FEBS Lett.* 383:105–108.

Lorand, L., N. G. Rule, H. H. Ong, R. Furlanetto, A. Jacobsen, J. Downey, N. Oner, and J. Bruner-Lorand. 1968. Amine specificity in transpeptidation. Inhibition of fibrin cross-linking. *Biochemistry.* 7:1214–1223.

Lorenz, M., D. Popp, and K. C. Holmes. 1993. Refinement of the F-actin model against x-ray fiber diffraction data by the use of a directed mutation algorithm. *J. Mol. Biol.* 234:826–836.

Ludescher, R. D., and Z. Liu. 1993. Characterization of skeletal muscle actin labeled with the triplet probe erythrosin-5-iodoacetamide. *Photochem. Photobiol.* 58:858–866.

Martonosi, A., and M. A. Gouvea. 1961. Studies on actin. VI. The interaction of nucleotide triphosphates with actin. *J. Biol. Chem.* 236: 1345–1352.

McLoughlin, P. J., J. T. Gooch, H.-G. Mannherz, and A. G. Weeds. 1993. Structure of gelsolin segment 1-actin complex and the mechanism of filament severing. *Nature.* 364:685–692.

Miki, M., and T. Kouyama. 1994. Domain motion in actin observed by fluorescence resonance energy transfer. *Biochemistry.* 33:10171–10177.

Moraczewska, J., H. Strzelecka-Gołaszewska, P. D. J. Moens, and C. G. dos Remedios. 1996. Structural changes in subdomain 2 of G-actin observed by fluorescence spectroscopy. *Biochem. J.* 317:605–611.

Mossakowska, M., J. Moraczewska, S. Khaitlina, and H. Strzelecka-Gołaszewska. 1993. Proteolytic removal of three C-terminal residues of actin alters the monomer-monomer interactions. *Biochem. J.* 289: 897–902.

Muhlrad, A., P. Cheung, B. C. Phan, C. Miller, and E. Reisler. 1994. Dynamic properties of actin. Structural changes induced by beryllium fluoride. *J. Biol. Chem.* 269:11852–11858.

Nagy, B., and W. P. Jencks. 1962. Optical rotatory dispersion of G-actin. *Biochemistry.* 1:987–996.

Newman, J., J. E. Estes, L. A. Selden, and L. C. Gershman. 1985. Presence of oligomers at subcritical actin concentration. *Biochemistry.* 24: 1538–1544.

Nowak, E., H. Strzelecka-Gołaszewska, and R. Goody. 1988. Kinetics of nucleotide and metal ion interaction with G-actin. *Biochemistry.* 27: 1785–1792.

Ooi, A., and K. Mihashi. 1996. Effects of subtilisin cleavage of monomeric actin on its nucleotide binding. *J. Biochem.* 120:1104–1110.

Orlova, A., and E. H. Egelman. 1992. Structural basis for the destabilization of F-actin by phosphate release following ATP hydrolysis. *J. Mol. Biol.* 227:1043–1053.

Orlova, A., and E. H. Egelman. 1993. A conformational change in the actin subunit can change the flexibility of the actin filament. *J. Mol. Biol.* 232:334–341.

Page, R., U. Lindberg, and C. E. Schutt. 1998. Domain motions in actin. *J. Mol. Biol.* 280:463–474.

Schutt, C. E., J. C. Myslik, M. D. Rozycki, N. C. W. Goonesekere, and U. Lindberg. 1993. The structure of crystalline profilin-beta-actin. *Nature.* 365:810–816.

Schwyter, D., M. Phillips, and E. Reisler. 1989. Subtilisin-cleaved actin: polymerization and interaction with myosin subfragment 1. *Biochemistry.* 28:5889–5895.

Selden, L. A., J. E. Estes, and L. C. Gershman. 1983. The tightly bound divalent cation regulates actin polymerization. *Biochem. Biophys. Res. Commun.* 116:478–485.

Spudich, J. A., and S. Watt. 1971. The regulation of rabbit skeletal muscle contraction. I. Biochemical studies of interaction of the tropomyosin-troponin complex with actin and the proteolytic fragments of myosin. *J. Biol. Chem.* 246:4866–4871.

Steinmetz, M. O., K. N. Goldie, and U. Aebi. 1997. A correlative analysis of actin filament assembly, structure, and dynamics. *J. Cell Biol.* 138: 559–574.

Strzelecka-Gołaszewska, H., J. Moraczewska, S. Y. Khaitlina, and M. Mossakowska. 1993. Localization of the tightly bound divalent-cation-dependent and nucleotide-dependent conformation changes in G-actin using limited proteolytic digestion. *Eur. J. Biochem.* 211:731–742.

Strzelecka-Gołaszewska, H., M. Mossakowska, A. Woźniak, J. Moraczewska, and H. Nakayama. 1995. Long-range conformational effects of proteolytic removal of the last three residues of actin. *Biochem. J.* 307:527–534.

Strzelecka-Gołaszewska, H., A. Woźniak, T. Hult, and U. Lindberg. 1996. Effects of the type of divalent cation, Ca^{2+}, or Mg^{2+} bound at the high-affinity site and of the ionic composition of the solution on the structure of F-actin. *Biochem. J.* 318:713–721.

Takashi, R. 1988. A novel actin label: a fluorescent probe at glutamine-41 and its consequences. *Biochemistry.* 27:938–943.

Tirion, M. M., and D. ben-Avraham. 1993. Normal mode analysis of G-actin. *J. Mol. Biol.* 230:186–195.

Tirion, M. M., D. ben-Avraham, M. Lorenz, and K. C. Holmes. 1995. Normal modes as refinement parameters for the F-actin model. *Biophys. J.* 68:5–12.

Valentin-Ranc, C., and M.-F. Carlier. 1991. Role of ATP-bound divalent metal ion in the conformation and function of actin. Comparison of Mg-ATP, Ca-ATP and metal ion-free ATP-actin. *J. Biol. Chem.* 266: 7668–7675.

West, J. J. 1971. Binding of nucleotide to cation-free G-actin. *Biochemistry.* 10:3547–3553.

Wriggers, W., and K. Schulten. 1996. Dynamics and stability of G-actin. *Biophys. J.* 70:A34.